Chinese Chemical Letters 37 (2026) 111204

Contents lists available at ScienceDirect

Chinese Chemical Letters

journal homepage: www.elsevier.com/locate/cclet

Rational engineering of an isoform-specific and sensitive turn-on estrogen sulfotransferase-activatable fluorescent probe for functional sensing and drug discovery

Xiaoting Niu[a,1], Yufan Fan[a,1], Lin Chen[a], Yanyan Deng[a], Yumeng Hao[a], Guanghao Zhu[a], Lixin Wang[a], Qihang Zhou[a], Guanghui Zhu[b,*], Guangbo Ge[a,*]

[a] State Key Laboratory of Discovery and Utilization of Functional Components in Traditional Chinese Medicine, Shanghai Frontiers Science Center of TCM Chemical Biology; Institute of Interdisciplinary Integrative Medicine Research, Shanghai University of Traditional Chinese Medicine, Shanghai 201203, China
[b] Department of Gastrointestinal Surgery, Shanghai Municipal Hospital of Traditional Chinese Medicine, Shanghai University of Traditional Chinese Medicine, Shanghai 200071, China

ARTICLE INFO

Article history:
Received 23 January 2025
Revised 9 April 2025
Accepted 13 April 2025
Available online 14 April 2025

Keywords:
SULT1E1
Fluorescent substrate
4-Hydroxyphenyl-1,8-naphthalimide
Functional sensing
Inhibitor screening

ABSTRACT

Estrogen sulfotransferase (SULT1E1), an essential conjugative enzyme in mammals, plays a crucial role in both estrogen homeostasis and xenobiotic metabolism. Deciphering the dynamic changes in SULT1E1 function under specific physiological or pathological conditions and discovering SULT1E1 modulators require practical and highly efficient tools for sensing SULT1E1 in biological context. Herein, we showcase a scaffold-seeking and structural optimization strategy for the rational engineering of isoform-specific fluorescent substrates for SULT1E1. First, docking-based virtual screening coupled with biochemical assays suggested that *N*–butyl–4-hydroxyphenyl-1,8-naphthalimide (HPN) was a suitable scaffold for constructing the fluorescent substrates for SULT1E1, but this fluorophore could be metabolized by multiple SULT isoforms. To develop isoform-specific substrates for SULT1E1, various substituents were introduced on the north part of HPN to explore the structure-enzyme specificity relationships of HPN derivatives as SULT1E1 substrates. After molecular docking and experimental validation, an isoform-specific fluorescent substrate (HPN10) for SULT1E1 was successfully engineered. HPN10 demonstrated exceptional isoform-specificity, ultra-high sensitivity, and favorable signal-to-noise ratio (212). HPN10 excelled in the precise sensing of SULT1E1 activities in complex biological matrices, including cellular specimens and liver preparations. HPN10 immensely facilitated the discovery and characterization of SULT1E1 inhibitors, while tetrabromobisphenol A (TBBPA, half inhibitory concentration (IC_{50}) = 31.5 ± 3.4 nmol/L) was identified as a potent SULT1E1 inhibitor that could strongly block SULT1E1 activities in living cells. Collectively, this work presents a practical and efficient strategy for the rational engineering of isoform-specific fluorescent substrates for target conjugative enzyme(s), while HPN10 emerges as a reliable SULT1E1-activatable tool for functional sensing and drug discovery.

© 2025 Published by Elsevier B.V. on behalf of Chinese Chemical Society and Institute of Materia Medica, Chinese Academy of Medical Sciences.

Mammalian sulfotransferases (SULTs), a key family of phase II conjugative enzymes, mediate essential biochemical transformations of both xenobiotic substances and endogenous metabolites [1–4]. Among all identified members of the human SULT family, estrogen sulfotransferase (SULT1E1) has drawn much attention, owing to this enzyme play crucial roles in the metabolic processing of both estrogens and therapeutic agents containing phenolic moieties. SULT1E1 effectively regulates the exposure levels of estrogens in the host by catalyzing the transfer of a sulfate group, typically from 3′-phosphoadenosine-5′-phosphosulfate (PAPS) to estrogens [5,6]. Specifically, SULT1E1 is responsible for the *O*-sulfation of estrogens (*e.g.*, estradiol and estrone), a key process that modulates the biological activities of estrogens and facilitates their excretion from the body [7–9]. It is well known that estrogens participate in numerous physiological processes (*e.g.*, reproductive function and metabolic regulation), and the activity levels of SULT1E1 in specific organs are key factors for maintaining hormonal balance and preventing estrogen-related disorders [10].

* Corresponding authors.
E-mail addresses: zhuguanghui@shutcm.edu.cn (G. Zhu), geguangbo@shutcm.edu.cn (G. Ge).
[1] These authors contributed equally to this work.

https://doi.org/10.1016/j.cclet.2025.111204
1001-8417/© 2025 Published by Elsevier B.V. on behalf of Chinese Chemical Society and Institute of Materia Medica, Chinese Academy of Medical Sciences.

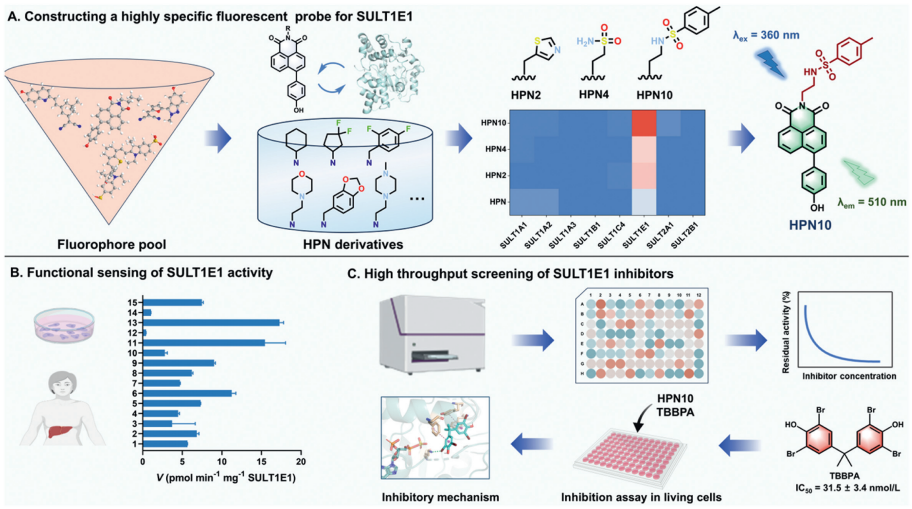
Dysregulation of SULT1E1 activity has been implicated in various diseases, including hormone-dependent cancers, metabolic disorders, and liver diseases [11,12]. In hormone-related cancers (*e.g.*, breast and endometrial cancers), the expression and activity levels of SULT1E1 are key factors affecting tumor growth and progression [13,14]. SULT1E1 also contributes significantly to the metabolism of exogenous estrogens, including the marketed selective estrogen receptor modulators (SERMs), such as tamoxifen and 17α-ethinylestradiol (EE) [5,8]. Pharmacological inhibition of SULT1E1 can strongly affect the treatment outcomes of the estrogenic drugs. SULT1E1 inhibitors have gained increasing attention in both basic research and drug development. Potent SULT1E1 inhibitors can elevate the circulating exposure levels of both endogenous and exogenous estrogens, enhancing their therapeutic effects [15]. Moreover, SULT1E1 inhibitors have been proposed as potential therapeutics for treating the disorders where estrogen plays protective or positive roles, such as metabolic diseases (*e.g.*, type 2 diabetes), inflammatory diseases (*e.g.*, sepsis), and acute kidney injury [16–19]. Selective modulation of SULT1E1 activity offers a targeted therapeutic strategy to restore estrogen-related signaling and ameliorate the metabolic disorders related to estrogen deficiency. The critical involvement of SULT1E1 in both disease pathogenesis and therapeutic outcomes underscores the importance of developing reliable activity assays and identifying potent inhibitors for targeted therapeutic interventions.

The development of reliable and practical tools for monitoring SULT1E1 activity in complex biological matrices is crucial for both deciphering its authentic biological roles and establishing its clinical relevance to human diseases. However, the previously reported methods for detecting SULT1E1 activity are limited by the lack of specific and practical tools. The previously reported assays for sensing SULT1E1 include immunoassays, liquid chromatography-tandem mass spectrometry (LC-MS/MS), radiolabeled substrate assays, and fluorescence detection using radiolabeled fluorine tags [20–25]. Immunoassays (*e.g.*, Western blot (WB) and enzyme-linked immunosorbent assay (ELISA)) are widely used for quantifying SULT1E1 expression, but they fail to detect the activity levels of SULT1E1. LC-MS/MS-based assays offer exceptional accuracy for detecting *O*-sulfation products in complex biological samples, but such assays are costly, labor-intensive, and incapable of high-throughput detection. Radiolabeled substrate assays show high sensitivity, but require radiolabeled compounds and can lead to environmental contamination. These limitations highlight the urgent need for developing more accessible, highly specific, and high-throughput-compatible tools to detect the activity levels of SULT1E1 in biological systems.

Enzyme-activatable fluorescent probes provide high sensitivity, enabling the real-time monitoring of enzyme activities with excellent spatial and temporal resolution [26,27]. Meanwhile, enzyme-activatable fluorogenic probes offer rapid and cost-effective assays for high-throughput screening of enzyme inhibitors, due to their compatibility with all devices equipped with a fluorescence detector (*e.g.*, microplate reader and liquid chromatography with fluorescence detection (LC-FD)). Unfortunately, isoform-specific SULT1E1-activatable fluorescent probes have not yet been reported, which greatly hinders the efficient sensing of the activity levels of SULT1E1 in living systems and high-throughput screening of SULT1E1 inhibitors.

This work aimed to develop an isoform-specific SULT1E1-activatable fluorescent probe, as well as to construct a highly efficient fluorescence-based assay for functional sensing of the real activities of SULT1E1 in complex biological samples and high-throughput screening inhibitors. For these purposes, a scaffold-seeking and structural optimization strategy was adopted to rational engineering of isoform-specific fluorescent substrates for SULT1E1. First, docking-based virtual screening suggested that *N*–butyl–4-hydroxyphenyl-1,8-naphthalimide (HPN) was a good substrate for SULT1E1, but this fluorophore could also be metabolized by other SULTs isoforms. To find the isoform-specific substrates for SULT1E1, various substitutes were introduced on the north part of HPN to explore the structure-enzyme specificity relationships of HPN derivatives as SULT1E1 substrates. Following structural optimization and experimental validation, an isoform-specific fluorescent substrate (HPN10) for SULT1E1 was successfully engineered (Scheme 1). HPN10 shows excellent isoform-specificity, rapid-responding, ultrahigh sensitivity, and is capable of high-throughput detection. HPN10 was subsequently applied for functional sensing of the activity levels of SULT1E1 in complex biological samples, including different human cell lines and human liver preparations. With the help of HPN10, a practical biochemical assay was constructed for high-throughput screening and characterization of SULT1E1 inhibitors, which was subsequently adopted for screening potent SULT1E1 inhibitors from synthetic and natural compounds.

Developing an isoform-specific fluorescent substrate for a target conjugative enzyme (such as a SULT isoform) is highly challenging. The first challenge arises from the high sequence homology between SULT1E1 and other SULT isoforms, making it difficult to achieve high isoform selectivity. The second challenge is that the fluorescence signals of most reported fluorescent agents bearing phenolic group are often quenched or blue-shifted following *O*-sulfation, which is unbeneficial for fluorescence detection. In fluorescent probes based on photoinduced electron transfer (PeT) or twisted intramolecular charge transfer (TICT), modifications on the recognition moiety by analytes typically disrupt the quenching process, leading to fluorescence recovery. This characteristic makes them particularly suitable for constructing the fluorescent probes of transferases. Inspired by existing transferase-activatable fluorescent probes, six structurally diverse fluorescent scaffolds were selected to test their potential as SULT1E1 substrates (Fig. S1 and Table S1 in Supporting information) [28–35]. After molecular docking, HPN was selected as a suitable scaffold for designing an isoform-specific fluorescent substrate for SULT1E1, owing to its high binding-affinity score and the high number of catalytic conformations formed. Biochemical assays showed that HPN could be metabolized by multiple SULT enzymes, including SULT1A1, SULT1A2, and SULT1E1 (Fig. 1A). Following sulfonation on the phenolic group, the PeT process was interrupted completely, resulting in a noticeable fluorescence recovery. Notably, the volume of the catalytic cavity of SULT1E1 (1255 Å^3) was much larger than that of SULT1A1 (796 Å^3) and SULT1A2 (784 Å^3), suggesting that SULT1E1 can accommodate more bulky substrates (Fig. 1B and Table S2 in Supporting information). Guided by this structural feature of SULT1E1, we designed ten HPN derivatives by modifying the north part of this fluorogenic scaffold (Fig. S2 in Supporting information). Molecular docking with SULT1E1 was performed to obtain the binding affinity scores and catalytic conformation for each HPN derivative. The results suggested that HPN2, HPN4, and HPN10 formed more catalytic conformations with SULT1E1 (Fig. 1C). These three agents were chemically synthesized and fully characterized (Schemes S1–S3 and Figs. S12–S29 in Supporting information), and their *O*-sulfation rates were tested individually. The results confirmed that the three synthesized HPN derivatives could be metabolized by SULT1E1, showing differential specificities over SULT1A1 (12.5-fold to 49.4-fold). Although HPN2 could distinguish SULT1A1 and SULT1E1 with high selectivity, SULT1C4 also catalyzed HPN2 *O*-sulfation. By contrast, HPN10 could be rapidly and specifically metabolized by SULT1E1 to form a mono *O*-sulfate, exhibiting excellent isoform selectivity (17.8-fold), rapid response and superior cell membrane permeability (Figs. 1D and E; Figs. S3, S4, S30–S33 and Scheme S4 in Supporting information). These results suggest that HPN10 emerges as an isoform-specific fluorogenic probe



Scheme 1. (A) Scaffold-seeking and structural optimization strategy for the rational engineering of isoform-specific fluorescent substrates for SULT1E1. (B) Functional sensing of SULT1E1 activities in complex biological samples using HPN10 as the fluorescent substrate. (C) Screening and characterization of SULT1E1 inhibitors using HPN10 as the fluorescent substrate.

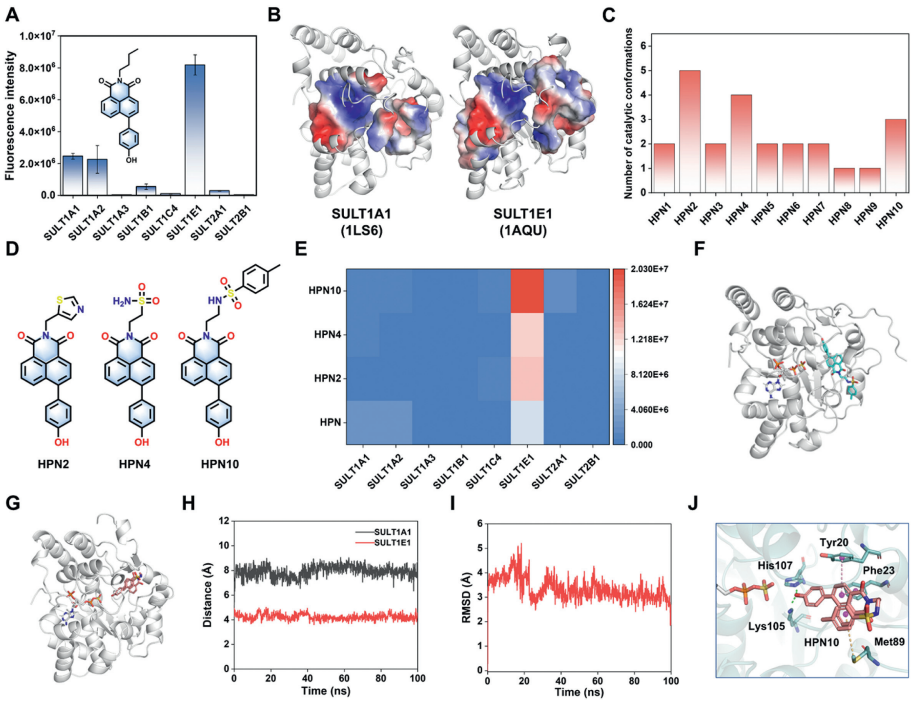


Fig. 1. Rational engineering of an isoform-specific fluorescent probe for SULT1E1. (A) Fluorescence response of HPN towards various human SULT isoforms (10 μg/mL). Data are presented as mean ± standard deviation (SD) ($n = 2$). (B) Comparison of the predicted catalytic pocket of SULT1A1 and SULT1E1. (C) The number of catalytic conformations of HPN derivatives docking with SULT1E1. (D) Structures of three synthesized HPN derivatives. (E) Sulfation phenotypic screening of the three synthesized HPN derivatives. MD simulations of HPN10 with SULT1A1 (F) and SULT1E1 (G), respectively. (H) Distance between the C-4 phenolic group on HPN10 and the sulfur atom of PAPS in SULT1A1 or SULT1E1 during 100 ns simulations. (I) The root mean square deviation (RMSD) of HPN10 in SULT1E1 during 100 ns simulations. (J) Binding and interaction patterns of HPN10 in SULT1E1.

for SULT1E1 through scaffold-seeking and structural optimization strategy.

Molecular dynamics (MD) simulations were conducted to explore the binding mechanism of HPN10 with SULT1E1. The results demonstrated that the distance between the C-4 phenolic group on HPN10 and the sulfur atom of PAPS in SULT1A1 was around 8 Å (Figs. 1F–H), while the distance between the C-4 phenolic group on HPN10 and SULT1E1 around 4 Å, indicating that HPN10 could readily form catalytic conformations within SULT1E1. The MD simulations results revealed that HPN10 could stably bind to the catalytic cavity of SULT1E1, forming strong and specific interactions with several key amino acids critical for substrate recognition and catalysis (Figs. 1I and J). Specifically, the oxygen atom of the C-4 phenolic group on HPN10 formed two hydrogen bonds with the Nε atom of Lys105 and the Nε2 of imidazole ring of His107, respectively, both of which are crucial for the catalytic activity of SULT1E1 [36,37]. Additionally, the naphthalene ring of HPN10 engaged in π-π stacking interactions with the aromatic residues Tyr20 and Phe23, further stabilizing the substrate-enzyme complex. These interactions collectively enhanced the binding affinity and specificity of HPN10 for SULT1E1, promoting its efficient metabolism.

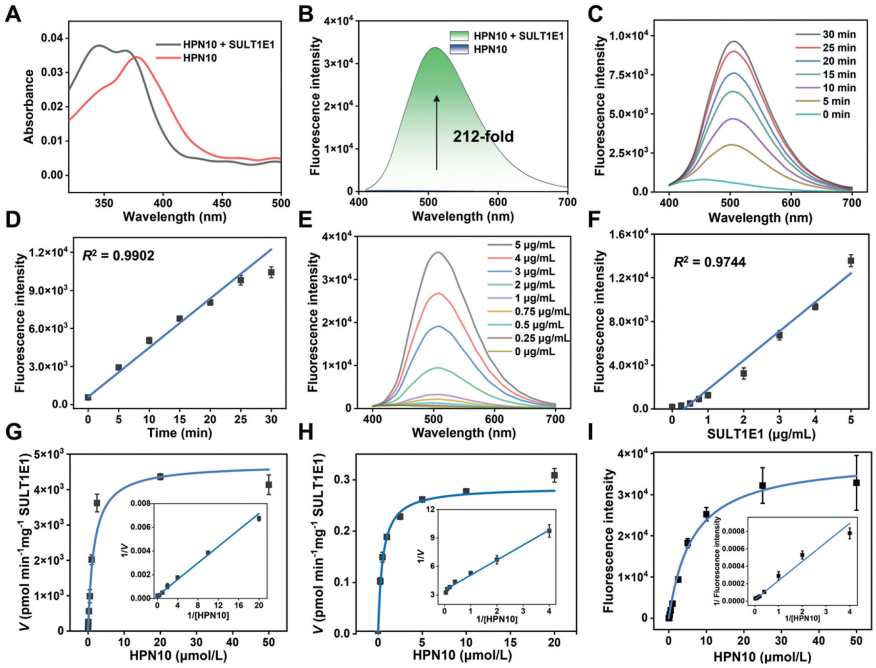


Fig. 2. Fluorescent properties of HPN10 towards SULT1E1. (A) Absorption spectra of HPN10 in the presence and absence of SULT1E1. (B) Fluorescence spectra of HPN10 with or without SULT1E1 ($\lambda_{ex}=360$ nm, $\lambda_{em}=510$ nm). (C) Time-dependent fluorescence spectra of HPN10 (1 μmol/L) after incubation with SULT1E1 (1 μg/mL) over 0–30 min. (D) Linear relationship between the reaction time and fluorescence intensity of HPN10 *O*-sulfate ($\lambda_{em}=510$ nm). (E) Fluorescence spectra of HPN10 (1 μmol/L) with increasing SULT1E1 concentrations (0.25–5 μg/mL) over 30 min. (F) Linear relationship between the SULT1E1 concentration and fluorescence intensity of HPN10 *O*-sulfate ($\lambda_{em}=510$ nm). (G–I) Kinetics of HPN10 *O*-sulfation in recombinant SULT1E1 (G), human liver S9 (H), and living MCF-7 cells (I), respectively. Inset: Lineweaver-Burk plots of HPN10 *O*-sulfation for different enzyme sources. Data are presented as mean ± SD ($n=3$).

Next, we thoroughly investigated the spectroscopic properties of HPN10 in the presence of SULT1E1. Upon the addition of SULT1E1, HPN10 exhibited a notable 'OFF–ON' fluorescence changes in a strong emission peak with a maximum wavelength of 510 nm (Figs. 2A and B and Table S3 in Supporting information). Under physiological conditions, the fluorescence intensity around 510 nm showed a linear response within 30 min incubation ($R^2=0.9902$) (Figs. 2C and D). Moreover, a linear response between the fluorescence intensity around 510 nm and the concentration of SULT1E1 was also observed within a range of 0.25–5 μg/mL ($R^2=0.9744$) (Figs. 2E and F). In addition, the fluorescence intensity was virtually undisturbed by endogenous amino acids, metal ions, and pH (Figs. S5 and S6 in Supporting information). These findings suggest that HPN10 is an ideal fluorogenic probe for precise and real-time monitoring of SULT1E1 activity, enabling its use in fundamental biochemical research and drug discovery applications.

Next, HPN10 *O*-sulfation kinetic analyses were investigated in various enzyme sources, including recombinant human SULT1E1 (Fig. 2G), human liver cytosol (Fig. 2H), and living MCF-7 cells (Fig. 2I). As shown in Figs. 2G–I and Table S4 (Supporting information), HPN10 *O*-sulfation catalyzed by human SULT1E1 followed canonical Michaelis-Menten kinetics, showing a Michaelis constant (K_m) of 1.67 ± 0.21 μmol/L and a V_{max} value of 4718.60 ± 426.60 pmol min^{-1} mg^{-1} SULT1E1. These findings demonstrated that HPN10 exhibited high binding affinity towards human SULT1E1 and a rapid *O*-sulfation rate. Notably, similar kinetic behavior was also observed for HPN10 *O*-sulfation catalyzed by human liver S9, with a K_m value of 0.52 ± 0.03 μmol/L. The comparable K_m values between recombinant SULT1E1 and human liver S9 suggest that SULT1E1 plays a predominant role in HPN10 *O*-sulfation in human liver S9. Additionally, the HPN10 *O*-sulfation kinetics was also investigated in living MCF-7 cells, showing canonical Michaelis-Menten kinetics and high apparent binding affinity (6.36 ± 0.85 μmol/L).

Subsequently, HPN10 was utilized to detect SULT1E1 activities in the various cell preparations from HepG2, MCF-7, and A549 cells. As shown in Fig. 3A and Fig. S7 (Supporting information), the total SULT1E1 activities in these cell preparations were highly correlated with cell counts. It is also observed that triclosan (a specific inhibitor of SULT1E1) strongly inhibited SULT1E1 activities in cell preparations, which further confirmed the pivotal role of SULT1E1 in HPN10 *O*-sulfation (Fig. 3B). It is well known that the activity levels of drug-metabolizing enzymes vary significantly among individuals, which can strongly affect drug efficacy and safety. Here,

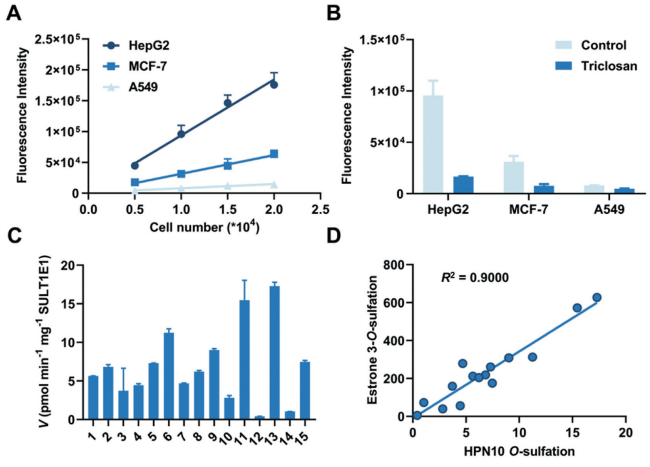


Fig. 3. Activity levels of SULT1E1 in biological samples using HPN10 as the substrate. (A) Linear fitting between the fluorescence intensity of SULT1E1-catalyzed HPN10 *O*-sulfation in the culture supernatant and the cell numbers of HepG2, MCF-7, and A549 cells. (B) Fluorescence intensity of SULT1E1-catalyzed HPN10 *O*-sulfation in HepG2, MCF-7, and A549 cells in the presence and absence of triclosan. (C) Fluorescence intensity of SULT1E1 in 15 individual samples from human liver cytosol. (D) Correlation analysis between HPN10 *O*-sulfation rates and estrone 3-*O*-sulfation rates in 15 individual human liver cytosol samples. Data are presented as mean ± SD ($n=3$).

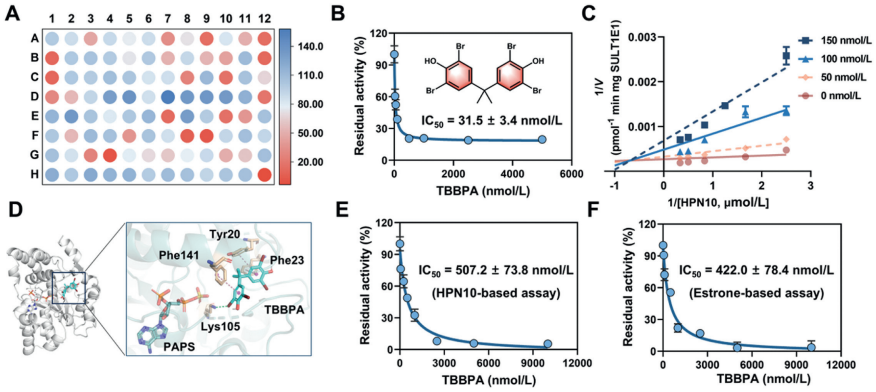


Fig. 4. High-throughput screening of SULT1E1 inhibitors. (A) The inhibitory effects of 96 compounds (10 μmol/L) against SULT1E1-catalyzed HPN10 *O*-sulfation. (B) Dose-dependent inhibition curve of TBBPA towards SULT1E1. (C) Inhibition kinetics of TBBPA against SULT1E1-catalyzed HPN10 *O*-sulfation. (D) Key interactions of TBBPA in SULT1E1. Dose-dependent inhibition curves of TBBPA against SULT1E1-catalyzed HPN10 *O*-sulfation (E) and estrone 3-*O* sulfation (F) in living MCF-7 cells. Data are presented as mean ± SD ($n = 3$).

HPN10 was applied to test the real SULT1E1 activities in human liver preparations. As shown in Figs. 3C and D and Table S5 (Supporting information), a remarkable 41.6-fold variation in SULT1E1 activity was observed among human liver cytosol samples from 15 individuals. This discrepancy was also validated by using estrone, a physiological substrate of SULT1E1 ($R^2 = 0.9000$). These observations suggest that HPN10 is a practical and specific tool for sensing SULT1E1 activities in complex biological matrices.

Given the pivotal role of SULT1E1 in both estrogen metabolism and xenobiotic detoxification processes, dysregulation of this critical conjugative enzyme may lead to significant disruptions in hormonal homeostasis [38–40]. To efficiently identify potent SULT1E1 inhibitors, we developed a fluorescence-based high-throughput screening assay using HPN10 as the probe substrate, which enabled rapid screening and precise characterization of SULT1E1 inhibitors. Triclosan (a previously reported SULT1E1 inhibitor) was used as a positive control to validate the applicability of this newly inhibition assay [24,41], showing the half inhibitory concentration (IC_{50}) of 279.3 nmol/L (Fig. S8 in Supporting information). After that, we screened the anti-SULT1E1 effects of a compound library containing natural and synthesized compounds. The results showed that three hormone analogs and endocrine-disrupting chemicals, including tetrabromobisphenol A (TBBPA), EE, and diethylstilbestrol, potently inhibited SULT1E1 with residual activity of $<10\%$ at a dose of 10 μmol/L (Fig. 4A and Table S6 in Supporting information). Among all tested agents, TBBPA showed the most potent anti-SULT1E1 effect, with the IC_{50} value of 31.5 ± 3.4 nmol/L (Fig. 4B and Fig. S9 in Supporting information). Subsequently, the anti-SULT1E1 mechanism of TBBPA was further investigated. As shown in Fig. 4C and Fig. S10 (Supporting information), TBBPA strongly inhibited SULT1E1 in a mixed competitive manner, with an inhibitory constant (K_i) of 48.25 nmol/L.

Molecule docking was further conducted to explore the binding mechanisms of this newly identified potent inhibitor of human SULT1E1. TBBPA could be well-docked into SULT1E1, showing a high binding affinity score (–8.1 kcal/mol). It was also observed that two phenyl rings of TBBPA strongly interacted with Tyr20, Phe23, and Phe141 *via* π-π stacking interactions (Fig. 4D), while the bromine atoms of TBBPA form stable interactions with Lys105. These observations partially explain why TBBPA could act as a strong inhibitor against human SULT1E1. After that, the inhibitory effect of TBBPA was further investigated in living MCF-7 cells (Figs. 4E and F, Fig. S11 in Supporting information). The results showed that TBBPA could potently inhibit SULT1E1 in a dose-dependent manner, with the IC_{50} value of 507.2 ± 73.8 nmol/L. Meanwhile, the inhibitory effect of TBBPA against SULT1E1 was also investigated in living MCF-7 cells using the physiological substrate estrone. TBBPA also displayed a potent inhibitory effect on SULT1E1-catalyzed estrone 3-*O*-sulfation in living MCF-7 cells. These findings suggest that TBBPA, an endocrine-disrupting chemical, can disturb the estrogenic homeostasis in living systems.

In summary, a novel turn-on fluorescent substrate (HPN10) of SULT1E1 was successfully constructed using a scaffold-seeking and structural optimization strategy. HPN10 showed exceptional isoform specificity, ultrahigh sensitivity, good cell membrane permeability, and favorable signal-to-noise ratio. HPN10 enabled sensing of SULT1E1 activities in various biological systems, including cellular specimens and tissue preparations. Using HPN10 as the probe substrate, a practical platform was constructed for high-throughput screening of SULT1E1 inhibitors, while TBBPA (an endocrine-disrupting chemical) was identified as a potent SULT1E1 inhibitor that could strongly block SULT1E1 activities in living cells. Collectively, this work presents a highly efficient strategy for rational engineering of a sensitive turn-on and isoform-specific fluorescent substrate for target conjugative enzyme(s), while HPN10 emerges as a practical and reliable SULT1E1-activatable tool for functional sensing and inhibitor screening that will greatly facilitate SULT1E1-related fundamental studies and translational research.

Declaration of competing interest

The authors declare that they have no known competing financial interests or personal relationships that could have appeared to influence the work reported in this paper.

CRediT authorship contribution statement

Xiaoting Niu: Writing – original draft, Methodology, Formal analysis. **Yufan Fan:** Methodology, Investigation. **Lin Chen:** Validation. **Yanyan Deng:** Validation. **Yumeng Hao:** Methodology. **Guanghao Zhu:** Software. **Lixin Wang:** Validation. **Qihang Zhou:** Methodology. **Guanghui Zhu:** Supervision, Resources. **Guangbo Ge:** Writing – review & editing, Supervision, Funding acquisition, Conceptualization.

Acknowledgments

This study was supported by Natural Science Foundation of China (Nos. U23A20516, 82273897, 81922070), Organizational Key Research and Development Program of Shanghai University of Traditional Chinese Medicine (No. 2023YZZ02), and the State Key Lab-

oratory of Fine Chemicals, Dalian University of Technology (Nos. KF2202, KF2414). Shanghai Municipal Health Commission's TCM research project (No. 2022CX005), Future Plan for Traditional Chinese Medicine development of Science and Technology of Shanghai Municipal Hospital of TCM (Nos. WL-XJRY-2021010 K, WL-GNDBZPY-2022001 K). Shanghai Jing'an District Health Commission (No. 2024QT03).

Supplementary materials

Supplementary material associated with this article can be found, in the online version, at doi:10.1016/j.cclet.2025.111204.

References

[1] M.W.H. Coughtrie, Chem. Biol. Interact. 259 (2016) 2–7.
[2] H. Glatt, Chem. Biol. Interact. 129 (2000) 141–170.
[3] H. Glatt, W. Meinl, Essays Biochem. 68 (2024) 523–539.
[4] M.W. Duffel, Essays Biochem 68 (2024) 541–553.
[5] M. Yi, M. Negishi, S.-J. Lee, J. Pers. Med. 11 (2021) 194.
[6] Y. Xu, X. Liu, F. Guo, et al., Cancer Sci. 103 (2012) 1000–1009.
[7] M.H. Kester, C.H. van Dijk, D. Tibboel, et al., J. Clin. Endocrinol. Metab. 84 (1999) 2577–2580.
[8] A.C.S. Barbosa, Y. Feng, C. Yu, M. Huang, W. Xie, Expert Opin. Drug Metab. Toxicol. 15 (2019) 329–339.
[9] H. Gong, M.J. Jarzynka, T.J. Cole, et al., Cancer Res. 68 (2008) 7386–7393.
[10] J. Wang, Y. Feng, B. Liu, W. Xie, Steroids 201 (2024) 109335.
[11] M. Fashe, M. Yi, T. Sueyoshi, M. Negishi, Biochem. Pharmacol. 190 (2021) 114662.
[12] E.B. Yalcin, V. More, K.L. Neira, et al., Drug Metab. Dispos. Biol. Fate Chem. 41 (2013) 1642–1650.
[13] J.R. Pasqualini, Ann. N. Y. Acad. Sci. 1155 (2009) 88–98.
[14] H. Hirata, Y. Hinoda, N. Okayama, et al., Cancer 112 (2008) 1964–1973.
[15] L. He, C. Chen, S. Duan, et al., J. Steroid Biochem. Mol. Biol. 225 (2023) 106182.
[16] A.C. Silva Barbosa, D. Zhou, Y. Xie, et al., J. Am. Soc. Nephrol. 31 (2020) 1496–1508.
[17] X. Chai, Y. Guo, M. Jiang, et al., Nat. Commun. 6 (2015) 7979.
[18] J. Gao, J. He, X. Shi, et al., Diabetes 61 (2012) 1543–1551.
[19] F. Mauvais-Jarvis, Diabetes 61 (2012) 1353–1354.
[20] G.B. Cole, G. Keum, J. Liu, et al., Proc. Natl. Acad. Sci. U. S. A. 107 (2010) 6222–6227.
[21] V.S. Parker, E.J. Squirewell, H.-J. Lehmler, L.W. Robertson, M.W. Duffel, Environ. Toxicol. Pharmacol. 58 (2018) 196–201.
[22] Z. Riches, E.L. Stanley, J.C. Bloomer, M.W.H. Coughtrie, Drug Metab. Dispos. 37 (2009) 2255–2261.
[23] C. Van Der Berg, G. Venter, F.H. Van Der Westhuizen, E. Erasmus, Anal. Biochem. 590 (2020) 113531.
[24] L.-Q. Wang, C.N. Falany, M.O. James, Drug Metab. Dispos. 32 (2004) 1162–1169.
[25] C. Xie, T.-M. Yan, J.-M. Chen, et al., Sci. Rep. 7 (2017) 3858.
[26] J. Zhang, X. Chai, X.-P. He, et al., Chem. Soc. Rev. 48 (2019) 683–722.
[27] H.W. Liu, L. Chen, C. Xu, et al., Chem. Soc. Rev. 47 (2018) 7140–7180.
[28] X. Lv, L. Feng, C.Z. Ai, et al., J. Med. Chem. 60 (2017) 9664–9675.
[29] Y. Liu, X. Wang, Z. Li, et al., Anal. Chem. 96 (2024) 7005–7013.
[30] S. Chen, X. Ma, L. Wang, et al., Sens. Actuat. B: Chem. 379 (2023) 133272.
[31] C. Yan, Z. Guo, W. Chi, et al., Nat. Commun. 12 (2021) 3869.
[32] L. Feng, J. Ning, X. Tian, et al., Coord. Chem. Rev. 399 (2019) 213026.
[33] L. Song, M. Sun, Y. Song, et al., Chin. Chem. Lett. 35 (2024) 109601.
[34] T. Sun, Z. Dong, P.M. Malugulu, et al., Chin. Chem. Lett. 36 (2025) 110451.
[35] H. Pan, X. Chai, J. Zhang, Chin. Chem. Lett. 34 (2023) 108321.
[36] Y. Kakuta, Lik.G. Pedersen, C.W. Carter, M. Negishi, L.C. Pedersen, Nat. Struct. Mol. Biol. 4 (1997) 904–908.
[37] S. Shevtsov, E.V. Petrotchenko, L.C. Pedersen, M. Negishi, Environ. Health Perspect. 111 (2003) 884–888.
[38] M.H. Kester, S. Bulduk, D. Tibboel, et al., Endocrinology 141 (2000) 1897–1900.
[39] R.Y. Jia, Z.P. Zhang, G.Q. Qin, et al., Environ. Pollut. Bark. Essex 1987 291 (2021) 118214.
[40] Z. Dai, F. Zhao, Y. Li, J. Xu, Z. Liu, Front. Endocrinol. 12 (2021) 814373.
[41] M.O. James, W. Li, D.P. Summerlot, L. Rowland-Faux, C.E. Wood, Environ. Int. 36 (2010) 942–949.